Spectroscopic, Thermodynamic and Molecular Docking Studies on Interaction of Toxic Azo Dye with Bovine Serum Albumin

N. Rasouli[b,*], N. Sohrabi[c], D. Ajloo[d] and N. Rezvani[a]

[a,b,c]*Department of Chemistry, Payame Noor University, P.O. Box: 19395-3697, Tehran, Iran*
[d]*School of Chemistry, Damghan University, Damghan, Iran*
(Received 6 January 2017, Accepted 26 April 2017)

Studies on interaction of azo dyes with bovine serum albumin, as carrier protein, would be of particular importance in the field of toxicology that can help in better understanding of dye-protein interaction mechanism. In this regard, the interaction between the azo dye, trisodium (4E)-3-oxo-4-[(4-sulfonato-1-naphthyl) hydrazono] naphthalene-2,7-disulfonate ($C_{20}H_{11}N_2Na_3O_{10}S_3$), known as Amaranth, and bovine serum albumin (BSA) was studied using UV-Vis absorption, fluorescence spectroscopy, viscosity measurement and molecular docking studies. Also, the association behavior of Amaranth was investigated at its various concentrations and different ionic strengths (NaCl) in 5 mM aqueous phosphate buffer of pH 7.0 at 25 °C. From the spectrophotometric studies, the binding constant was determined. The value of the binding constant was $K_b = 0.71 \times 10^4$ M^{-1} at 298 K. Thermodynamic parameters ($\Delta H > 0$ and $\Delta S > 0$) indicated that hydrophobic forces play a major role in the interaction between Amaranth and BSA. From the results of fluorescent experiments, the binding constants and the number of binding sites were obtained as $K_b = 3.4 \times 10^7$ M^{-1} and 1.2901, respectively. By increasing the amount of Amaranth, a significant increase in viscosity of BSA was observed. The molecular docking method was employed to understand the interaction of Amaranth with BSA. The results showed that BSA has great affinity for interaction with Amaranth dye.

Keywords: Toxic Azo dye, Bovine serum albumin, Thermodynamic, Fluorescence quenching, Molecular docking

INTRODUCTION

Recently, much research has been carried out on the dyes due to their extensive usage in the various industries such as textile, dyeing, paper, printing, pharmaceutical, food and cosmetics [1,2]. The azo dyes containing azo (-N=N-) functional groups and aromatic structure are used in about half of all dyes that reductively cleaved into aromatic amines with toxic, mutagenic and carcinogenic properties. Amaranth (FD & C Red No. 2, E123, C. I. Food Red 9) (Fig. 1) is a reddish or brownish azo dye which is used as a color additive in foodstuffs, pharmaceuticals and cosmetics. Amaranth dye, as an azo colorant, was reported to be potentially toxic to human [3], therefore there is a necessary need to control the consumption of this dye. Generally, the

physiological and toxicological properties of dyes are related to their binding nature to the biological macromolecules such as proteins, hence, the study on the interaction of proteins with dyes becomes important [4,5]. Serum albumins are known as the most abundant carrier proteins in blood plasma with many important physiological functions. The properties such as absorption, distribution, metabolism and excretion as well as the stability and toxicity of chemicals can be changed significantly because of their binding to serum albumin. Therefore, studying the interaction of serum albumin with chemicals is important to understand their transport and mechanism in body [6]. In this study, we have used bovine serum albumin (BSA) as a protein model due to low cost, availability, intrinsic fluorescence emission and structural homology with human serum albumin (HSA) [7]. BSA is composed of three linearly arranged and structurally homologous sub-
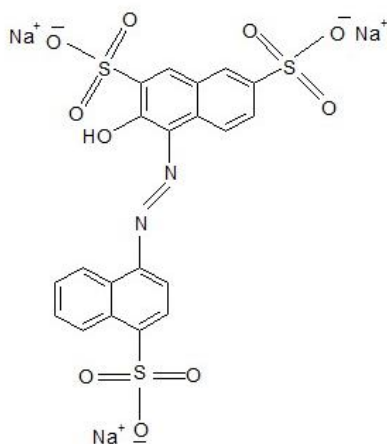
———————
*Corresponding author. E-mail: n.rasouli@pnu.ac.ir
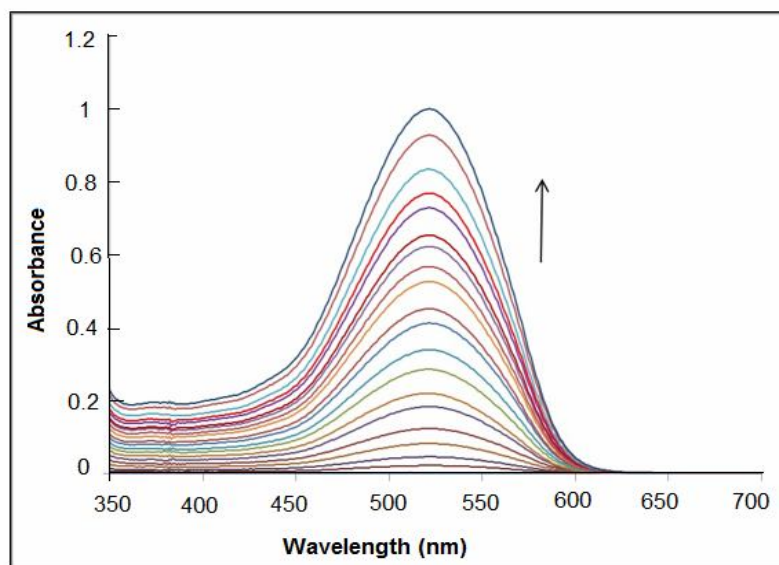
Fig. 1. The Chemical structure of Amaranth.

Fig. 2. UV-Vis absorption spectra of Amaranth in the concentration range from 2.9×10^{-7}-6.3×10^{-5} M in 5 mM phosphate buffer, pH 7 at 25 °C.

domains. It has two tryptophan residues possessing intrinsic domains (I-III) that each domain is the product of two fluorescence Trp-134 and Trp-212, located on the surface of sub-domain IB and IIA, respectively [8,9]. The main sites of drug binding in serum albumin protein are often located in hydrophobic cavities in sub-domains IIA and IIIA. The binding of a ligand to serum albumin affects the secondary and tertiary structure of serum albumin protein [10]. Up to

now, the effect of Amaranth on bovine serum albumin (BSA), specially using molecular docking has not been reported. To the best of our knowledge, the binding mechanisms of Amaranth to BSA protein remain unclear. So, in the present study, the binding of Amaranth (Fig. 1) to bovine serum albumin (BSA) and the consequent conformational changes are investigated in view of thermodynamics using UV-Vis absorption, fluorescence

spectroscopy and molecular docking method. Spectroscopic and molecular docking results are used to understand the mechanism of interactions.

EXPERIMENTAL

Materials

Bovine serum albumin (BSA) and Amaranth were purchased from Sigma-Aldrich chemical company. All experiments were performed in 5 mM phosphate buffer at pH 7.0, and at 25 °C. The buffer solution includes (339.44 mg l^{-1} $Na_2HPO_4.2H_2O$ and 426.8 mg l^{-1} $NaH_2PO_4.H_2O$) dissolved in the double distilled water.

UV-Vis Absorption

The absorbance measurements were carried out using UV-Vis, Perkin Elmer Lambda 25 double beam Spectrophotometer, operating from 200 to 700 nm in 1.0 cm quartz cells at room temperature.

Fluorescence Study

The fluorescence spectra were carried out on a Shimadzu model RF-5000 spectrofluorimeter equipped with a xenon lamp source and 1 cm quartz cell. The excitation wavelength was set at 280 nm and the fluorescence intensity was measured at 350 nm. The scan speed was 1200 nm/min.

Viscosity Measurement

The viscosity of BSA solutions was measured using an Ostwald viscometer at 25 ± 0.1 °C.

Molecular Docking Studies

In order to find out the binding sites on BSA, and the binding energy, molecular docking studies were performed. The structure of ligand was generated by Gauss View, version 4.1.2 followed by energy minimization. The crystal structure of BSA with PDB ID 4F5S was obtained from Protein Data Bank (http://www.rcsb.org). All water molecules and ligand were removed, and then hydrogen atoms were added to the protein structure. The molecular docking calculations were carried out using Auto Dock 4.2 software [11]. For the identification of the binding sites on BSA, docking studies were performed using a box size of 126 × 106 × 126 Å with grid resolution of 0.71 Å. The

docking runs were carried out using Auto Dock engine with a maximum of 200 candidate poses, and Amaranth was selected as a flexible ligand. The conformations were ranked using the A scoring function, which estimates the free binding energy. After molecular docking calculations, the ligand-protein interaction was further analyzed using Pymol 2.0.

RESULTS AND DISCUSSION

The UV-Vis Absorption Spectroscopy

The UV-Vis absorption measurement is a very simple and applicable method to understand the structural changes and the ligand-protein interactions. The UV-Vis absorption spectrum of Amaranth is characterized by strong absorption band in the visible region (λ_{max} = 522 nm) that is responsible for the red color of Amaranth [12] (Fig. 2). To check compliance with the Beer-Lambert law, the experiment was carried out in homogeneous aqueous solution in 5 mM aqueous phosphate buffer of pH 7.0 at 25 °C. The results showed that the absorption in λ_{max} = 522 nm, and concentration range of 0.0-6.3 × 10^{-5} M follow from the Beer's law (Fig. 3). Therefore, the Amaranth dye do not aggregate in the experimental concentration range. The effect of NaCl on the absorption spectrum of the Amaranth in aqueous solution is shown in Fig. 4. As the concentration of NaCl increases from 7.1 × 10^{-7} to 2.3 × 10^{-5} M, the absorption spectrum of Amaranth shows no significant electrolyte effect, and no new band appears even at high concentrations of NaCl. These results indicate that Amaranth do not form any aggregates. The change of ionic strength is an efficient method for distinguishing the binding modes between protein and other molecules. The high ionic strength was advantageous to the hydrophobic process but disadvantageous to the electrostatic binding [13]. Figure 5 shows the effect of NaCl concentration on the interaction of BSA with Amaranth. As seen in Fig. 5, the wavelength of maximum absorption of the Amaranth do not show considerable changes by increasing of NaCl concentration. As the concentration of NaCl increases, the absorbance exhibits hypochromism, therefore, the electrostatic force is very weak in the interaction between BSA and Amaranth. The UV-Vis absorption spectra of Amaranth in the absence and presence of different concentrations of BSA are
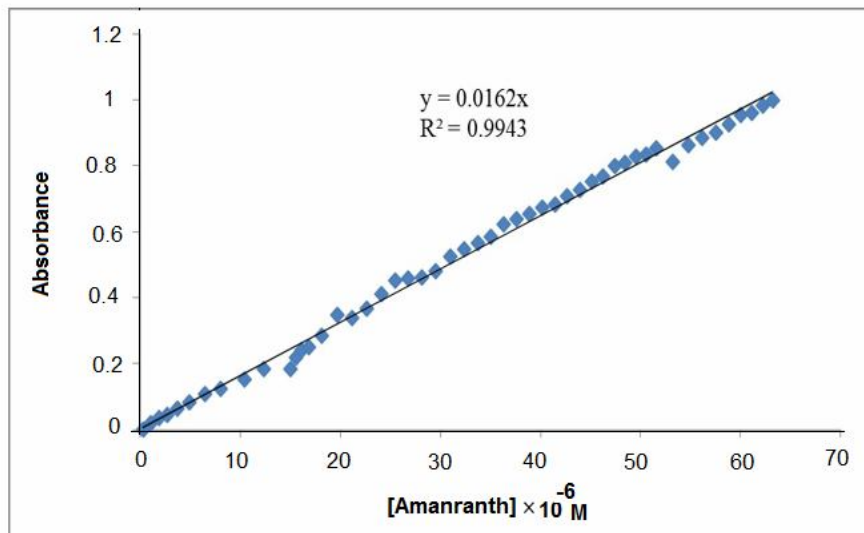
Fig. 3. The absorption spectra of Amaranth at the $\lambda_{max} = 522$ nm in the concentration range of 0-6.3 × 10^{-5} M in 5 mM phosphate buffer, pH 7 at 25 °C followed by Beer's law.

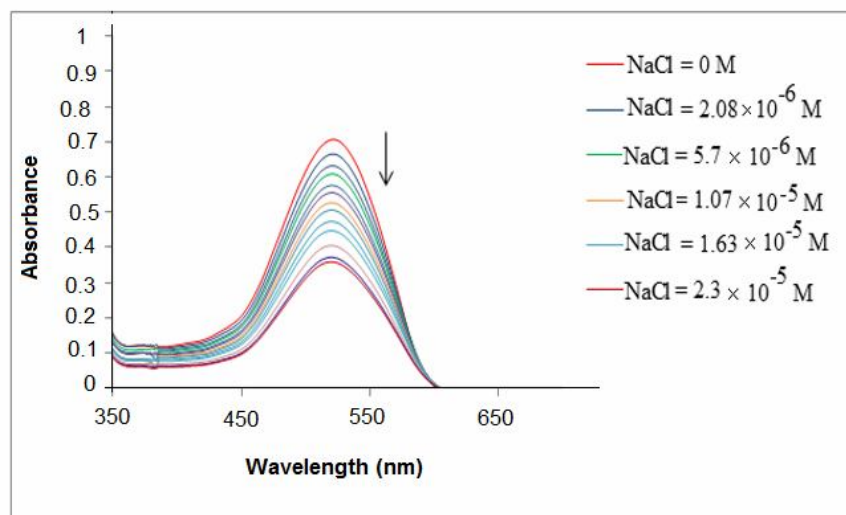**Fig. 4.** UV-Vis absorption spectra of Amaranth (4.8 × 10^{-5} M) at various concentration of NaCl (7.1 × 10^{-7} M- 2.3 × 10^{-5} M) in 5 mM phosphate buffer, pH 7 at 25 °C.

illustrated in Fig. 6. Upon addition of BSA, the absorbance and its intensity at 522 nm decreased and the peak position showed a slight shift to higher wavelengths, suggesting the strong interaction between Amaranth and BSA. Also, the observed isosbestic points at 307 nm and 566 nm proved the formation of the new complexes between BSA and Amaranth. The binding strength of Amaranth with BSA (K_b) was obtained by monitoring the changes in the Amaranth absorbance at 522 nm by increasing of BSA concentrations according to the following equation [14].
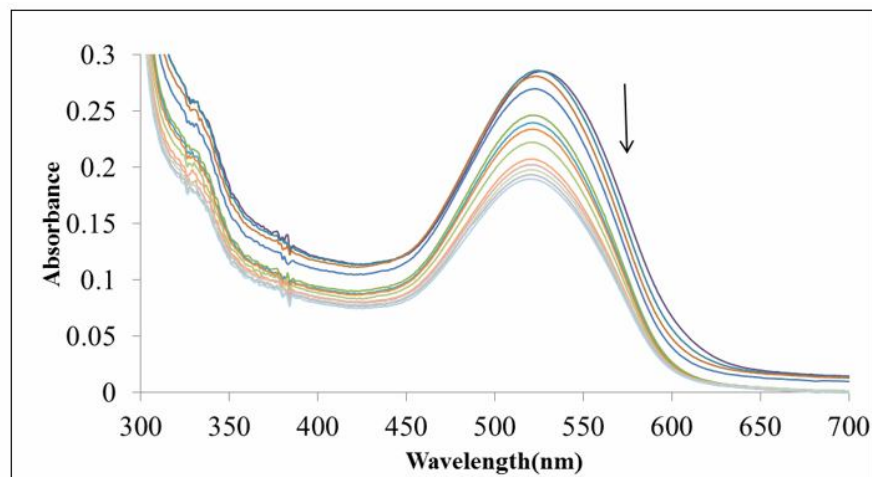
Fig. 5. UV-Vis absorption spectrum of BSA/Amaranth complex solution upon addition of NaCl (3 M) in 5 mM phosphate buffer, pH 7.0 and at 25 °C.
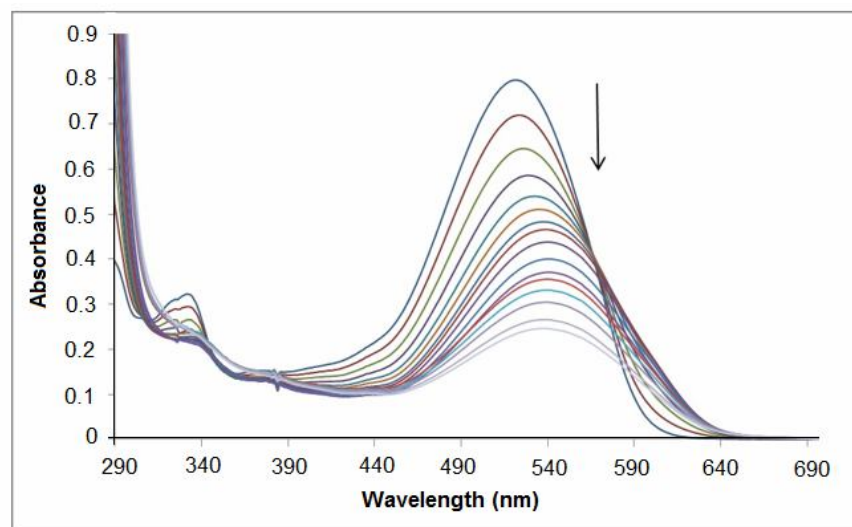

Fig. 6. UV-Vis absorption spectrum of Amaranth (5.5×10^{-5} M) in the presence of various concentrations of BSA in 5 mM phosphate buffer, pH 7 at 25 °C.

$$[BSA]/(\varepsilon_a - \varepsilon_f) = [BSA](\varepsilon_b - \varepsilon_f) + 1/K_b\,(\varepsilon_b - \varepsilon_f) \qquad (1)$$

where [BSA] is the concentration of BSA, ε_a, ε_f, and ε_b are the apparent extinction coefficient, and the extinction coefficient for the free and bound complex absorptivity, respectively. In the plots of $[BSA]/(\varepsilon_a - \varepsilon_f)$ *vs*. [BSA], K_b was given by the ratio of the slope to intercept (Fig. 7). The

apparent binding constant was calculated to be 0.71×10^4 M^{-1}.

Fluorescence Quenching Studies

BSA has a strong intrinsic fluorescence originating from the tryptophan (Trp), tyrosine (Tyr) and phenylalanine (Phe) residues [15]. When BSA protein interacts with various
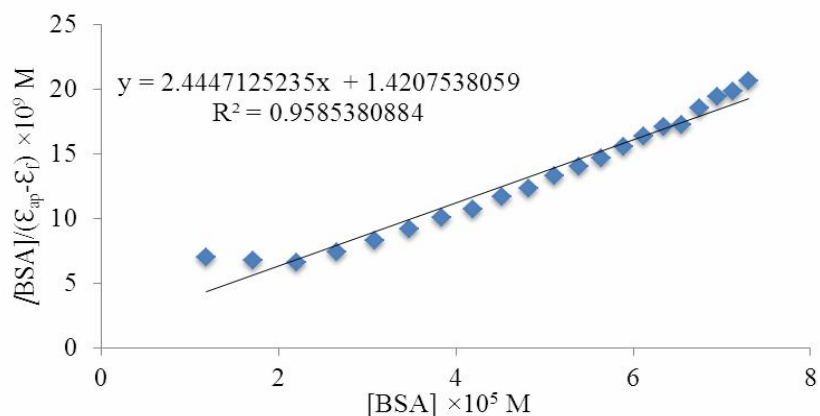
Fig. 7. The plot of $[BSA]/(\varepsilon_{aP} - \varepsilon_f)$ *vs*. $[BSA]$.
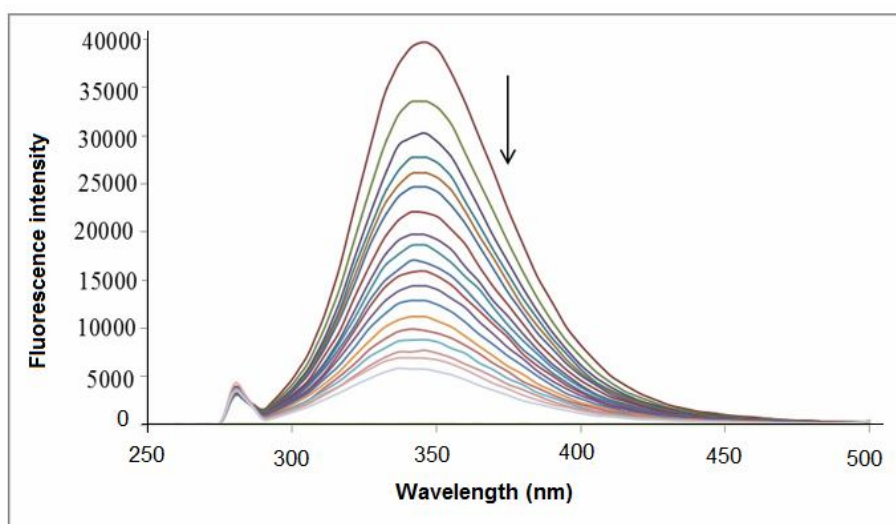

Fig. 8. Fluorescence spectrum of BSA (3×10^{-6} M) in the presence of various concentrations of Amaranth in 5 mM phosphate buffer, pH 7 at 25 °C.

compounds, its intrinsic fluorescence changes with the compound concentration. Consequently, fluorescence can be considered as a useful technique for determining the mechanism of interaction between compounds and BSA [16]. Figure 8 shows the fluorescence spectra of BSA in the presence of various concentrations of Amaranth. The results showed that BSA has a strong fluorescence emission peak at about 350 nm, and its fluorescence intensity decreases regularly with addition of various concentrations of Amaranth. To determine the mechanism of binding between

Amaranth and BSA, the fluorescence intensity data were analyzed by the Stern-Volmer equation (Eq. (2)) [17]:

$$F_0/F = 1 + Ksv\,[Q] \tag{2}$$

where F_0 and F are the fluorescence intensities in the absence and presence of quencher, respectively, K_{sv} is the Stern-Volmer quenching constant, and $[Q]$ is the concentration of quencher. In Fig. 9, the plot of F_0/F *vs*. $[Q]$ exhibits a good linear relationship, indicating the static
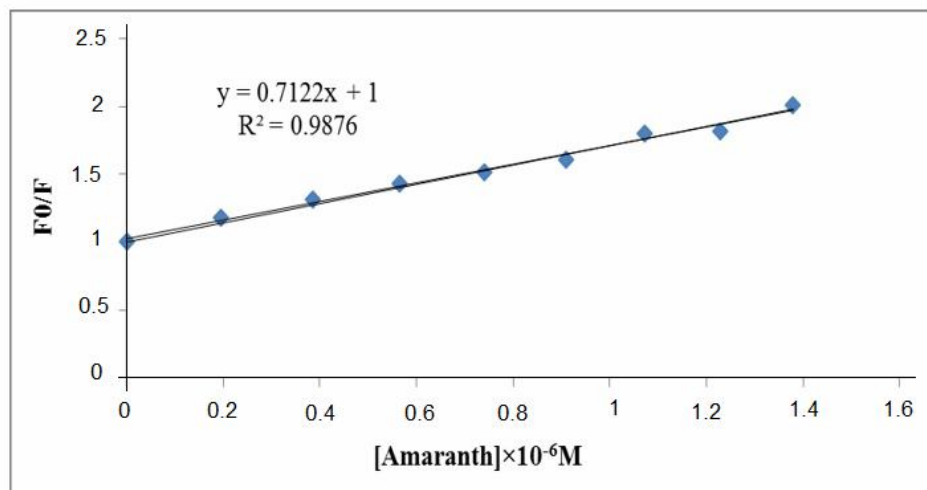
Fig. 9. Fluorescence quenching curve BSA (3×10^{-6} M) by Amaranth at $\lambda_{max} = 350$ nm in 5 mM phosphate buffer, pH 7 at 25 °C.
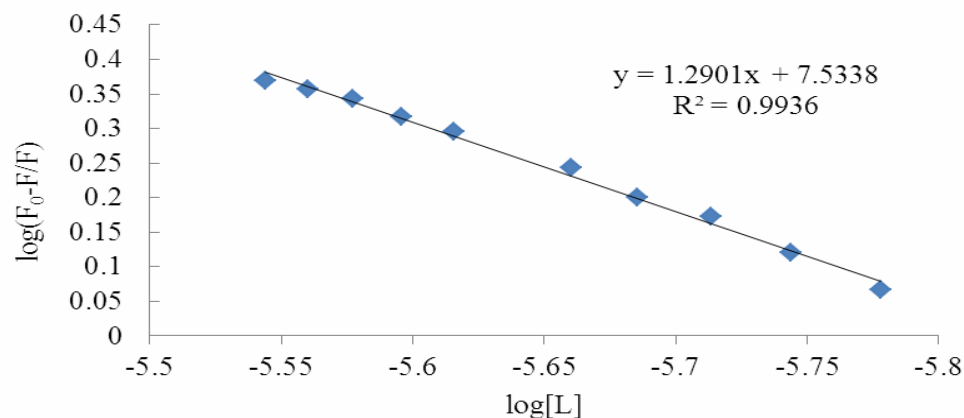

Fig. 10. Double log plots of Amaranth binding to BSA in 5 mM phosphate buffer, pH 7 at 25 °C.

quenching process, while, the deviation from linear relationship showed the presence of both static and dynamic quenching [18]. According to the Stern-Volmer equation and our experimental results, the Stern-Volmer quenching constant was 0.7122 M^{-1} s^{-1} at room temperature (Fig. 9).

Determination of Binding Constant and the Number of Binding Sites

 The binding constant (K_b) and the number of binding sites (n) can be calculated by the double logarithm regression curve (Fig. 10). The relationship between the fluorescence intensity and the quenching medium can be deduced by the Eq. (3):

$$\log(F_0\text{-}F/F) = \log K_b + n \log[Q] \tag{3}$$

where F_0 and F represent the fluorescence intensity without or with the quencher. [Q] is the concentration of the quencher. The values of binding constant, K_b, and binding sites, n, for interaction of Amaranth with BSA were
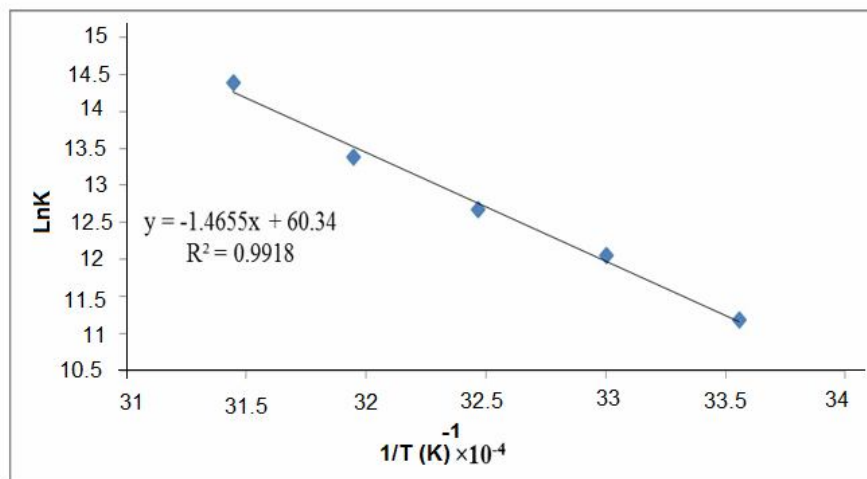
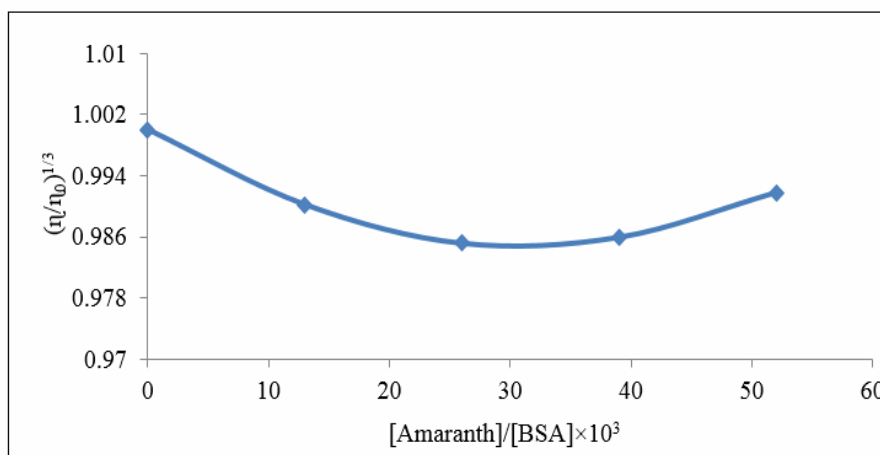**Fig. 11.** The Van't Hoff plot for the binding of BSA to Amaranth.

Fig. 12. Effect of increasing amounts of Amaranth on the viscosity of BSA (1.26×10^{-5} M) in 5 mM phosphate buffer, pH 7 at 25 °C at various molar ratios (R = 0.0, 0.013, 0.026, 0.039, 0.052).

obtained from the intercept and slope, respectively (Fig.10). The value of K_b is 3.4×10^7 M^{-1} at room temperature, indicating that a strong interaction exists between Amaranth and BSA. Also, the binding site value approximately equals 1.2901, which can be concluded that there is one binding site in BSA for interaction with Amaranth.

Thermodynamic Parameters of Binding

The thermodynamic parameters of binding are the main parameters for the binding force confirmation. Based on the thermodynamic definitions, $\Delta H > 0$ and $\Delta S > 0$ show hydrophobic interaction, $\Delta H < 0$ and $\Delta S > 0$ indicate an electrostatic force, $\Delta H < 0$ and $\Delta S < 0$ suggest the van der Waals force and hydrogen bonding [19]. When the change of temperature is small, ΔH can be considered a constant and the thermodynamic parameters of the binding reaction are as follows, Eqs. (4) and (5):

Table 1. Thermodynamic Parameters of Amaranth-BSA Interaction at pH 7.0

T (K)	lnK	$\Delta G°$ (kJ mol^{-1})	$\Delta S°$ (J mol^{-1} K^{-1})
298	11.18 ± 0.115	-27.70 ± 12.63	503.08 ± 20.85
303	12.05 ± 0.036	-30.36 ± 12.73	503.57 ± 20.85
308	12.67 ± 0.11	-32.44 ± 12.84	502.15 ± 20.85
313	13.38 ± 0.044	-34.82 ± 12.94	501.74 ± 20.85
318	14.38 ± 0.083	-38.03 ± 13.05	503.92 ± 20.85

Table 2. Effect of Increasing Amounts of Amaranth on the Viscosity of BSA (1.26×10^{-5} M) in 5 mM Phosphate Buffer, pH 7 at 25 °C at Various Molar Ratios (R = 0.0, 0.013, 0.026, 0.039, 0.052)

Solution	ρ (g ml^{-1})	T (s)	η (cP)
Water	0.998	97.45	1000
BSA	0.989	94.51	961.59
BSA (0.013)	0.984	92.25	933.65
BSA (0.026)	0.985	90.77	919.39
BSA (0.039)	0.991	90.4	921.59
BSA (0.052)	0.997	91.49	938.05

$$\ln K_a = -\Delta H/RT + \Delta S/R \qquad (4)$$

$$\Delta G = \Delta H - T \Delta S \qquad (5)$$

where K_b is the binding constant at the corresponding temperature, and R is the gas constant. Using the plot of ln K_b *vs*. 1/T, $\Delta H°$ and $\Delta S°$ are determined (Fig. 11). The thermodynamic parameters ($\Delta H°$, $\Delta S°$ and $\Delta G°$) for the interaction of Amaranth with BSA are summarized in Table 1. As reported in this table, $\Delta H°$ and $\Delta S°$ for the binding of Amaranth to BSA are 122.21 kJ mol^{-1} and 503.08 J mol^{-1} K^{-1} at 298 K, respectively. The negative value of $\Delta G°$ means that the binding process is spontaneous. We applied this analysis to the binding of Amaranth to BSA and found that

$\Delta H > 0$ and $\Delta S > 0$. Therefore, hydrophobic forces are the main forces involved in the binding process [20].

Viscosity

Hydrodynamic data such as viscosity measurement, as an effective test, were used for understanding the binding mode [21]. A complete or partial intercalation binding led to an increase of protein viscosity. In contrast, there is a little effect on the viscosity of protein if electrostatic or covalent binding occurs in the binding process [22,23]. In this regard, to understand the nature of BSA binding of the Amaranth, viscosity measurements were carried out on BSA by varying the concentration of the added Amaranth. The values of relative specific viscosity (η/η_0), where η and η_0 are the
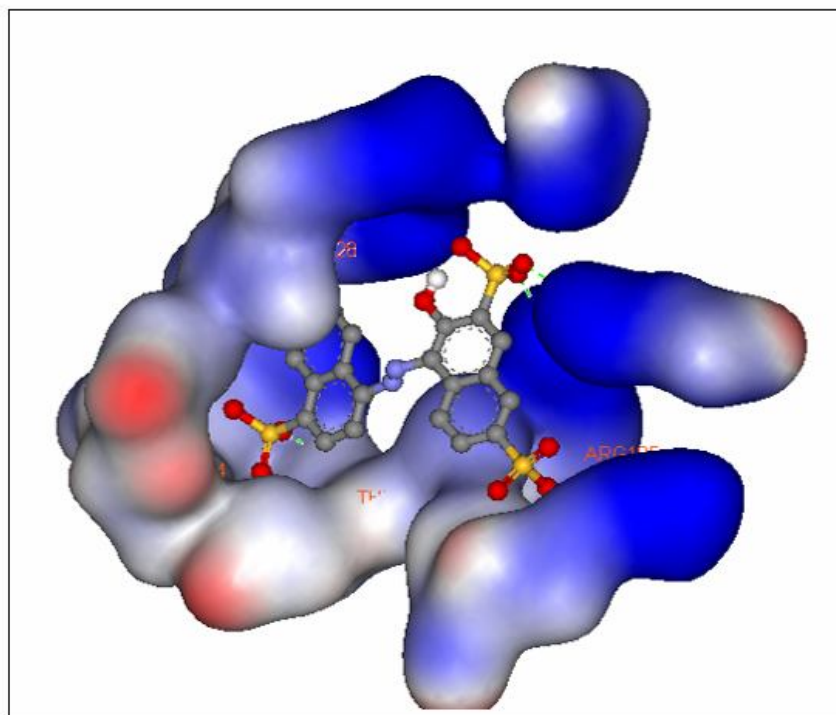
Fig. 13. The best conformation of the binding mode between Amaranth and BSA.
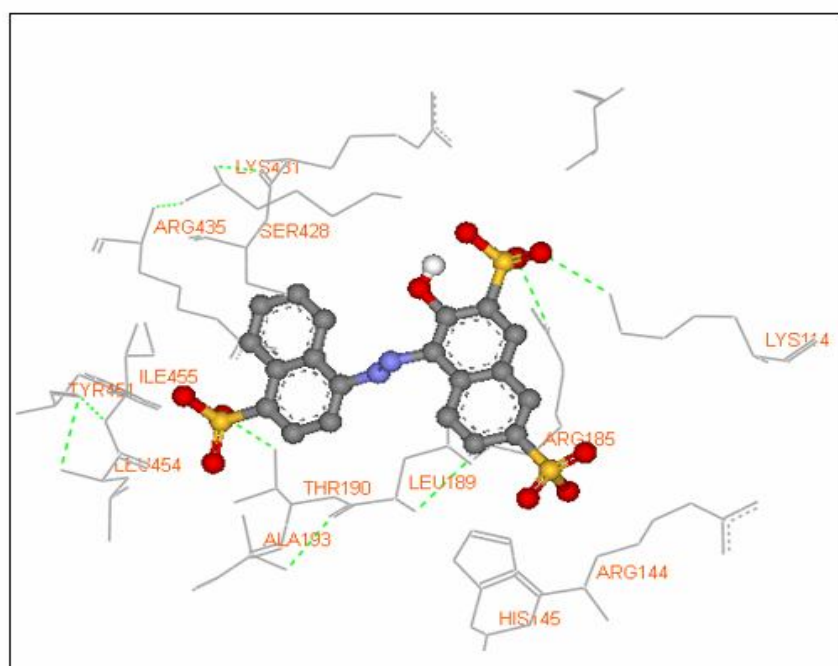

Fig. 14. The formation of hydrogen bonds between Amaranth and amino acid residues of BSA.

Table 3. Docking Energies in kcal mol^{-1} for Binding of Amaranth to BSA

Cluster rank	Docking energies	Number of run in a cluster	Cluster rank	Docking energies	Number of run in a cluster	Cluster rank	Docking energies	Number of run in a cluster
1	-9.54	9	28	-6.58	2	55	-5.73	1
2	-9.45	5	29	-6.58	2	56	-5.72	2
3	-8.6	10	30	-6.57	1	57	-5.71	2
4	-8.11	14	31	-6.51	3	58	-5.71	1
5	-8.07	2	32	-6.46	4	59	-5.7	2
6	-7.92	2	33	-6.45	1	60	-5.66	2
7	-7.89	2	34	-6.38	3	61	-5.65	1
8	-7.74	1	35	-6.35	4	62	-5.61	1
9	-7.39	2	36	-6.33	6	63	-5.6	1
10	-7.37	1	37	-6.3	3	64	-5.56	1
11	-7.35	6	38	-6.28	1	65	-5.56	1
12	-7.29	6	39	-6.2	1	66	-5.49	1
13	-7.27	2	40	-6.16	3	67	-5.49	1
14	-7.19	2	41	-6.15	1	68	-5.48	3
15	-7.09	1	42	-6.12	2	69	-5.47	1
16	-7.05	2	43	-6.07	1	70	-5.4	1
17	-7.01	5	44	-5.96	4	71	-5.24	1
18	-6.96	17	45	-5.96	1	72	-5.22	1
19	-6.95	1	46	-5.95	1	73	-5.1	1
20	-6.86	4	47	-5.95	1	74	-5.1	1
21	-6.83	1	48	-5.91	2	75	-5.02	1
22	-6.83	7	49	-5.89	1	76	-4.92	1
23	-6.78	1	50	-5.88	1	77	-4.87	1
24	-6.66	2	51	-5.86	1	78	-4.85	1
25	-6.64	3	52	-5.81	2	79	-4.81	1
26	-6.61	1	53	-5.8	1	80	-4.68	1
27	-6.59	4	54	-5.79	1	81	-4.64	1

specific viscosities of BSA in the presence and absence of the Amaranth, respectively, are plotted against [Amaranth]/ [BSA] (Fig. 12). It can be seen that the relative viscosity of BSA decreased with increasing the Amaranth concentration (Table 2). It is thought that the hydrophobic groups such as sulfonate in the Amaranth structure interact preferentially with the surface of protein molecules and participate in breaking the three-dimensional protein networks, thereby reducing solution viscosity [24].

Molecular Docking

In this research, Auto Dock 4.2 software, as a useful computational molecular docking program, was used to understand the interaction of Amaranth with BSA. The fluorescence and UV-Vis spectroscopic results were completed with molecular docking in which Amaranth was docked into BSA to determine the preferred binding site and the binding mode. There are two drug binding grooves located in BSA protein, namely as binding site I and site II, respectively, which are present in the hydrophobic cavities of sub domain IIA and IIIA. Figure 13 shows the best conformation of the binding mode between Amaranth and BSA. It is recognizable that Amaranth binds within the site I of sub-domain IIA pocket in domain II of BSA. Figure 14 illustrates hydrogen bonds between Amaranth and amino acid residues of BSA. Amaranth forms hydrogen bonds with GLU-152, SER-191, HIS-287, LYS-221, ARG-217, ARG-194 and VAL-292 residues. Furthermore, Amaranth is surrounded by three amino acid residues of TYR-149, ARG-198 and LYS-294. The binding energy for the Amaranth–BSA complex were calculated from the docking calculations and presented in Table 3. The number of runs in a cluster from negative to less negative values are shown in Table 3. Positions of 81 cluster ranks, most negative rank, surrounded amino acids and related surface charge were investigated. The results showed that the most negative cluster is near the positive amino acids. On the other hand, those cluster ranks located near Trp 134 and 213 with energies of -7.39 kcal mol^{-1} for rank 9 and -4.92 for rank 7 and 6 are also observed. So, the ligand tends to locate close to the Trp134.

CONCLUSIONS

In this research, the interaction of Amaranth with BSA was investigated by fluorescence, and UV-Vis spectroscopies under physiological conditions. Also, the molecular docking studies were carried out. The results obtained from the fluorescence showed that Amaranth quenches the intrinsic fluorescence of BSA *via* static quenching, and that there is a single class of binding site on BSA. The results of thermodynamic studies showed that the interaction process is spontaneous and is driven by entropy parameter. According to the molecular docking results, Amaranth can bind to BSA at site I in subdomain IIA. On the basis of the experimental results, it is inferred that there is a strong interaction between Amaranth and BSA.

ACKNOWLEDGEMENTS

REFERENCES

[1] Hunger, K., Industrial Dyes Chemistry, Properties, Applications. Wiley-VCH Verlag GmbH & Co, Weinheim, 2003.

[2] Erkurt, H. A., The Handbook of Environmental Chemistry, Biodegradahttp://refhub.elsevier.com/ S0022-2313(13)00350-5/sbref2tion of Azo Dyes. Springer-Verlag, Berlin, 2010.

[3] Mpountoukas, P.; Pantazaki, A.; Kostarelib, E.; Christodouloub, P.; Karelia, D.; Polilioua, S.; Mourelatosa, C.; Lambropouloua, V.; Lialiaris, T., Cytogenetic evaluation and DNA interaction studies of the food colorants amaranth, erythrosine and tartrazine. *Food Chem. Toxicol.* **2010**, *48*, 2934-2944, DOI: 10.1016/j.fct.2010.07.030.

[4] Ding, F.; Zhao, G.; Chen, Sh.; Liu, F.; Sun,Y.; Zhang, L., Chloramphenicol binding to human serum albumin: Determination of binding constants and binding sites by steady-state fluorescence. *J. Mol. Struct.* **2009**, *929*, 159-166, DOI: org/10.1016/ j.molstruc.2009.04.018.

[5]   Tang, J.; Qi, S.; Chen, X., Spectroscopic studies of the interaction of anti-coagulant rodenticide diphacinone with human serum albumin. *J. Mol. Struct.* **2005**, *779*, 87-95, DOI: org/10.1016/ j.molstruc.2005.07.023.

[6]   Sathyadevi, P.; Krishnamoorthy, P.; Alagesana, M.; Thanigaimanib, K.; Thomas Muthiahb, P.; Dharmaraj, N., Synthesis, crystal structure, electrochemistry and studies on protein binding, antioxidant and biocidal activities of Ni(II) and Co(II) hydrazone complexes. *Polyhedron* **2012**, *31*, 294-306, DOI: org/10.1016/j.poly.2011.09.021.

[7]   Zhang, S. L.; Damu, G. L. V.; Zhang, L.; Geng, R. X.; Zhou, C. H., Synthesis and biological evaluation of novel benzimidazole derivatives and their binding behavior with bovine serum albumin. *Eur. J. Med. Chem.* **2012**, *55*, 164-175, DOI:.org/10.1016/ j.ejmech.2012.07.015.

[8]   Anbazhagan, V.; Renganathan, R., Study on the binding of 2,3-diazabicyclo[2.2.2]oct-2-ene with bovine serum albumin by fluorescence spectroscopy. *J. Lumin.* **2008**, *128*, 1454-1458, DOI: org/10.1016/ j.jlumin.2008.02.004.

[9]   Pershin, G. N.; Sherbakova, L. I.; Zykova, T. N., Antibacterial activity of pyrimidine and pyrrolo-(3,2-d)-pyrimidine derivatives. *Farmakol. Toksikol.* **1972**, *35*, 466-471.

[10] Oravcova, J.; Bobs, B.; Lindner, W., Drug-protein binding studies new trends in analytical and experimental methodology. *J. Chromatogr. B: Biomed. Sci. Appl.* **1996**, *677*, 1-28, DOI: org/ 10.1016/0378-4347 (95) 00425-4.

[11] Morris, G. M.; Goodsell, D. S.; Halliday, R. S.; Huey, R.; Hart, W. E.; Belew, R. K.; Olson, A. J., Automated docking using a Lamarckian genetic algorithm and an empirical binding free energy function. *J. Comput. Chem.* **1998**, *19*, 1639-1662, DOI: 10.1002/(SICI) 1096-987X(19981115)19: 14<1639::AID-JCC10>3.0.CO;2-B.

[12] Basu, A.; Kumar, G. S., Interaction of toxic azo dyes with heme protein: biophysical insights into the binding aspect of the food additive amaranth with human hemoglobin. *J. Hazard. Mater.* **2015**, *289*, 204-209, DOI: org/10.1016/j.jhazmat.2015.02.044.

[13] Otzen, D. E.; Protein unfolding in detergents: effect of micelle structure, ionic strength, pH, and temperature. *Biophysics, J.* **2002**, *83*, 2219-2230, DOI: org/ 10.1016%2FS0006-3495(02)73982-9.

[14] Nejat Dehkordi, M.; Bordbar, A. K.; Lincoln, P.; Mirkhani, V., Spectroscopic study on the interaction of ct-DNA with manganese Salen complex containing triphenyl phosphonium groups. *Spectrochim. Acta A Mol. Biomol. Spectrosc.* **2012**, *90*, 50-54, DOI: 10.1016/j.saa.2012.01.015.

[15] Papadopoulou, A.; Green, R. J.; Frazier, R. A., Interaction of flavonoids with bovine serum albumin: a fluorescence quenching study. *J. Agric. Food. Chem.* **2005**, *53*, 158-163, DOI: org/10.1021/ jf048693g.

[16] Chi, Z.; Liu, R.; Teng, Y., Binding of oxytetracycline to bovine serum albumin: spectroscopic and molecular modeling investigations. *J. Agric. Food. Chem.* **2010**, *58*, 10262-10269, DOI: 10.1021/ jf101417w.

[17] Lakowicz, J. R., Principles of Fluorescence Spectroscopy, 3nd ed, Springer. New York, 2006.

[18] Thipperudrappa, J.; Biradar, D. S.; Lagare, M. T.; Hanagodimath, S. M.; Inamdar, S. R.; Kadadevaramath, J. S., Fluorescence quenching of BPBD by aniline in benzene-acetonitrile mixtures. *J. Photochem. Photobiol. A: Chem.* **2006**, *177*, 89-93, DOI: org/10.1016/j.jphotochem.2005.05.016

[19] Wu, S. S.; Yuan, W.B.; Zhang, Q.; Wang, H. Y.; Liu, M.; Yu, K. B., Synthesis, crystal structure and interaction with DNA and HSA of (N,N'-dibenzylethane-1,2-diamine) transition metal complexes. *J. Inorg. Biochem.* **2008**, *102*, 2026-2034, DOI: 10.1016/j.jinorgbio.2008.08.005.

[20] Hemmateenejad, B.; Shamsipour, M., Samari, F.; Khayamian, T.; Ebrahimi, M.; Rezaei, Z., Combined fluorescence spectroscopy and molecular modeling studies on the interaction between harmalol and human serum albumin. *J. Pharm. Biomed. Anal.* **2012**, *67*, 201-208, DOI: org/10.1016/j.jpba.2012.04.012.

[21] Satyanarayana, S.; Dabrowiak, J. C.; Chaires, J. B., Tris (phenanthroline) ruthenium(II) enantiomer interactions with DNA: Mode and specificity of

binding. *Biochem.* **1992**, *31*, 9319-9324, DOI: 10.1021/bi00061a015.

[22] Lerman, L. S., Structural considerations in the interaction of DNA and acridines. *J. Mol. Biol.* **1961**, *3*, 18-30, DOI: 10.1016/B978-0-12-131200-8.50008-3.

[23] Zhang, G.; Fu, P.; Pan, J., Multispectroscopic studies of paeoniflorin binding to calf thymus DNA *in vitro*.

J. Lumin. **2013**, *134*, 303-309, DOI: org/10.1016/j.jlumin.2012.08.029.

[24] Liu, J.; Nguyen, M. D.; Andya, J. D.; Shire, S. J., Reversible self-association increases the viscosity of a concentrated monoclonal antibody in aqueous solution. *J. Pharm. Sci.* **2005**, *94*, 1928-1940, DOI: 10.1002/jps.20347.